

## Review

**Biophysical aspects of blood flow in the microvasculature<sup>1</sup>**A.R. Pries<sup>a,\*</sup>, T.W. Secomb<sup>b</sup>, P. Gaehtgens<sup>a</sup><sup>a</sup> *Department of Physiology, Freie Universität Berlin, Arnimallee 22, D-14195 Berlin, Germany*<sup>b</sup> *Department of Physiology, University of Arizona, Tucson, AZ 85724, USA*

Received 12 December 1995; accepted 1 February 1996

**Abstract**

The main function of the microvasculature is transport of materials. Water and solutes are carried by blood through the microvessels and exchanged, through vessel walls, with the surrounding tissues. This transport function is highly dependent on the architecture of the microvasculature and on the biophysical behavior of blood flowing through it. For example, the hydrodynamic resistance of a microvascular network, which determines the overall blood flow for a given perfusion pressure, depends on the number, size and arrangement of microvessels, the passive and active mechanisms governing their diameters, and on the apparent viscosity of blood flowing in them. Suspended elements in blood, especially red blood cells, strongly influence the apparent viscosity, which varies with several factors, including vessel diameter, hematocrit and blood flow velocity. The distribution of blood flows and red cell fluxes within a network, which influences the spatial pattern of mass transport, is determined by the mechanics of red cell motion in individual diverging bifurcations. Here, our current understanding of the biophysical processes governing blood flow in the microvasculature is reviewed, and some directions for future research are indicated.

**Keywords:** Microcirculation; Blood flow; Viscosity; Red blood cells

**1. Introduction**

The microvasculature of a perfused tissue provides a large area for exchange of materials, and brings blood into close proximity with each point in the tissue. The architecture of the microvasculature and the biophysical behavior of the blood flowing through it strongly influence its capacity for material transport and exchange. Blood is a concentrated suspension of cells in plasma, and mechanical interactions between blood cells and the microvasculature affect the distribution of blood flow within networks of microvessels and the overall resistance to flow.

The biophysics of blood flow in microvessels has been studied for many years, using a number of different approaches, including *in vivo* and *in vitro* experimental studies and theoretical models. Previous reviews include those of Gaehtgens [1], Chien [2], Zweifach and Lipowsky [3], Goldsmith et al. [4] and Secomb [5]. In the present review, the focus is on the mechanics and hemodynamics of blood flow in the microvasculature. Coverage of this

area is, however, not complete. The biophysics of leukocyte and platelet interactions with microvessels, exchange of macromolecules and oxygen, and blood flow regulation are not discussed, since most of these areas are addressed elsewhere in this issue. Here, some biophysical properties of the blood are first reviewed. Then, the mechanics of blood flow in individual vessels, in bifurcations, and in networks of vessels are considered. Developments within the last 10–15 years are emphasized, with brief mention of earlier studies. Finally, implications for network hemodynamics, and directions for future work are discussed.

**2. Mechanical properties of blood cells**

The hematocrit of normal human blood is about 45%, and so red blood cells strongly influence the flow properties of blood. The basic mechanical properties of human red blood cells are well established [6,7]. The cytoplasm is an incompressible, Newtonian fluid. It is surrounded by a thin viscoelastic membrane, which consists of a lipid bilayer and a protein cytoskeleton. The membrane shears and

\* Corresponding author. Tel. (+49-30) 8 38 20 87; Fax (+49-30) 8 38 49 16.

<sup>1</sup> Supported by Deutsche Forschungsgemeinschaft (Ga 225/5-3, Pr 271/1-1, 1-2 and 5-1) and by NIH Grant HL34555.

Time for primary review 28 days.

bends easily (elastic shear modulus  $\approx 0.006$  dyn/cm, bending modulus  $\approx 1.8 \times 10^{-12}$  dyn/cm) but resists area changes (modulus of isotropic dilation  $\approx 500$  dyn/cm). A Kelvin solid model can be used for the viscoelastic behavior of the membrane in shear deformations, with the total stress represented as the sum of viscous and elastic contributions [8]. As a consequence of these properties, red cells are highly deformable, as long as changes in surface area or volume are not required, and can pass through capillaries with diameters much less than the diameter of an unstressed cell (8  $\mu\text{m}$ ).

Blood of many species, including human blood, can exhibit aggregation. Unless fluid flow forces are sufficient to keep them dispersed, red cells tend to adhere to each other due to bridging by plasma proteins [9]. In bulk shear flow, aggregation increases blood viscosity at low shear rates. As the shear rate is increased, the progressive breakup of aggregates leads to a decrease in viscosity ('shear thinning'). Increasing deformation of red cells with increasing shear rate also contributes to this trend, which is observed over a wide range of shear rates [9].

Other types of blood cells, including white blood cells and platelets, normally represent a very small volume fraction of blood. However, white blood cells are much stiffer than red cells, and may contribute significantly to microvascular flow resistance [10]. Platelets are much smaller than red cells, and do not contribute significantly to flow resistance.

### 3. Blood flow in microvessels

The finite size of red blood cells strongly influences the flow properties of blood in tubes with diameters less than about 300  $\mu\text{m}$ . Mechanical interactions between red cells and tube walls generally result in the formation of a plasma layer or a region of reduced hematocrit adjacent to the wall, and increased concentration of red cells near the center of the tube. This effect, termed 'axial migration' [11,12], has significant consequences for the overall flow behavior of blood in narrow tubes, including dynamic reduction of intravascular hematocrit (Fahraeus effect), and reduction of flow resistance below the level that would be expected based on the bulk viscosity of blood (Fahraeus-Lindqvist effect). The effects of aggregation on flow resistance in narrow tubes can also be quite different from its effects in bulk flow. These phenomena have been studied extensively in vitro and have been modeled theoretically, but their significance for blood flow in living tissue is less well understood.

#### 3.1. Fahraeus effect

Fluid flow velocity varies from zero at the wall of a tube to a maximum near the center. Therefore, red cell velocity and concentration are positively correlated within

each vessel cross-section, and average red cell velocity ( $v_c$ ) is higher than average blood velocity ( $v_b$ ). This leads to a reduction of red cell transit time through a given tube segment, and hence to a reduction of the hematocrit contained in that segment (tube hematocrit,  $H_T$ ) relative to the hematocrit of blood entering or leaving it (discharge hematocrit,  $H_D$ ), according to the equation [13]

$$\frac{H_T}{H_D} = \frac{v_b}{v_c} \quad (1)$$

This dynamic hematocrit reduction is generally known as the Fahraeus effect [14].

For a parabolic velocity profile with a ratio between maximal flow velocity in the center of a tube and the mean flow velocity of 2, the theoretical lower bound for  $H_T/H_D$  is 0.5 (for zero hematocrit). In the presence of red cells, this bound is shifted upwards due to the higher volume fraction occupied by the cells and due to blunting of the velocity profile. For discharge hematocrits of about 0.4, experimental investigations of tube flow [13–15] yielded minimal values for the quotient  $H_T/H_D$  of about 0.7 at diameters ranging from 20  $\mu\text{m}$  down to 10  $\mu\text{m}$ . At smaller tube diameters,  $H_T/H_D$  increases again towards unity. These characteristics of the dependence of the Fahraeus effect on tube diameter ( $D$ ) and discharge hematocrit are included in the parametric description

$$\frac{H_T}{H_D} = H_D + (1 - H_D) \cdot (1 + 1.7 e^{-0.415D} - 0.6 e^{-0.011D}) \quad (2)$$

compiled by Pries et al. [16] for model simulations of blood flow.

#### 3.2. Fahraeus-Lindqvist effect

Beginning with the investigations of Martini et al. [17] and Fahraeus and Lindqvist [18] it became evident that the flow resistance of blood during tube flow cannot be predicted on the basis of the viscosity of the blood as measured in large scale viscometers and the hydraulic resistance of the tube: the blood viscosity derived from volume flow rate at a given driving pressure using Poiseuille's law decreased with decreasing diameter of the tubes employed in the experiments. Obviously, this measure of blood viscosity does not solely reflect a material property of the blood, but rather a property of the blood/tube system at given flow conditions and has therefore been called 'apparent viscosity' or 'effective viscosity'. A large number of publications has addressed the dependence of apparent blood viscosity on tube diameter, hematocrit, and flow velocity. For medium to high flow velocities (above 50 tube diameters/s) the results of 18 studies were combined to a parametric description of apparent blood viscosity relative to the viscosity of plasma ('relative apparent vis-

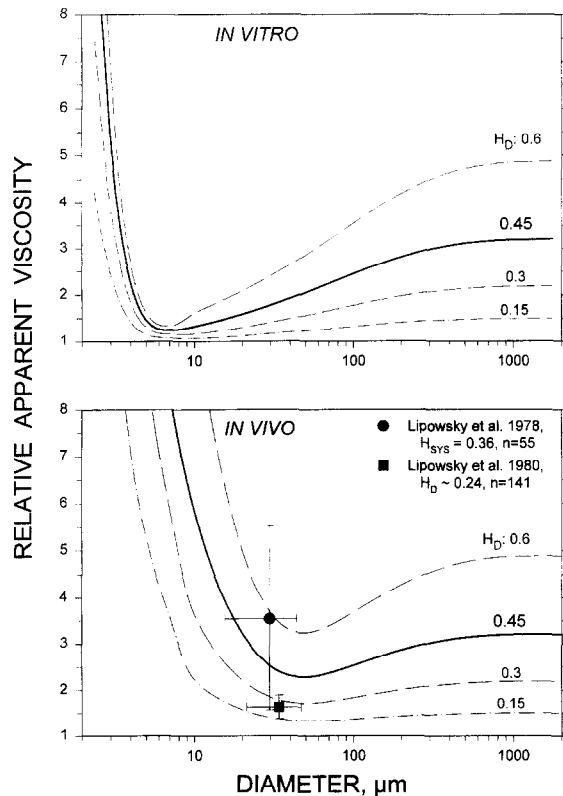


Fig. 1. Relative apparent viscosity of blood. *Upper*: Parametric description of results from 18 in vitro studies on tube flow of blood (cited in [19]). *Lower*: Relative apparent blood viscosity in vivo determined by network analysis in the mesentery [25] compared to results of direct measurements by Lipowsky et al. [23,24]. Equations for the parametric descriptions are given in the text.

cosity') as a function of tube diameter and hematocrit (Fig. 1) [19] according to the equation,

$$\eta_{vitro} = 1 + (\eta_{0.45} - 1) \cdot \frac{(1 - H_D)^C - 1}{(1 - 0.45)^C - 1} \quad (3)$$

Here  $\eta_{0.45}$ , the relative apparent blood viscosity for a fixed discharge hematocrit of 0.45, is given by

$$\eta_{0.45} = 220 \cdot e^{-1.3D} + 3.2 - 2.44 \cdot e^{-0.06D^{0.645}} \quad (4)$$

and  $C$  describes the shape of the viscosity dependence on hematocrit

$$C = (0.8 + e^{-0.075D}) \cdot \left( -1 + \frac{1}{1 + 10^{-11} \cdot D^{12}} \right) + \frac{1}{1 + 10^{-11} \cdot D^{12}} \quad (5)$$

The apparent blood viscosity exhibits a strong decrease with decreasing tube diameter reaching a minimum at about 7  $\mu\text{m}$ . In this diameter range, the apparent viscosity of blood with a discharge hematocrit of 0.45 is only 25% higher than that of cell-free plasma, indicating a very weak hematocrit dependence. Only at diameters below about 3.5  $\mu\text{m}$  does the apparent viscosity increase above the level seen in large vessels.

### 3.3. Theoretical basis for Fahraeus and Fahraeus-Lindqvist effects

The existence of a red-cell-depleted layer adjacent to the tube wall underlies both the Fahraeus and the Fahraeus-Lindqvist effects. Its effect may be illustrated using the 'stacked-coins' (or 'axial-train') model for blood flow [20]. In this model, all red cells are assumed to lie in a cylindrical core region of diameter  $\lambda D$  on the axis of a tube of diameter  $D$ . The core is assumed to move as a rigid body. The velocity profile is a blunted parabola, and it can be shown that

$$\frac{H_T}{H_D} = \frac{1 + \lambda^2}{2} \quad \text{and} \quad \eta_{vitro} = \frac{1}{1 - \lambda^4} \quad (6)$$

The ratio  $H_T/H_D$  decreases as the width of the plasma layer increases (decreasing  $\lambda$ ), and approaches 0.5 as  $\lambda$  approaches zero. Because of the fourth power dependence in the denominator of the latter expression, even a narrow plasma layer leads to a relatively low value of  $\eta_{vitro}$ . For instance, if  $\lambda = 0.8$  then  $\eta_{vitro} = 1.7$ , which is much less than relative bulk viscosity of whole blood, even though this equation gives an overestimate, due to the assumption that the core moves as a rigid body.

The actual width of the cell-free or cell-depleted layer depends in a complex way on the mechanics of individual red blood cells and their interactions with solid boundaries in flow. A general theoretical description of this behavior has not been developed. However, some progress has been made for the case of single-file motion of red cells, such as frequently occurs in capillaries with diameters of 6  $\mu\text{m}$  or less. The cells are deformed into shapes that are narrower than the capillary. Their motion may be analyzed theoretically, assuming axisymmetric cell shapes and using lubrication theory to describe the plasma flow in the gap between the cell and the wall. For tube diameters ranging from 3  $\mu\text{m}$  to 8  $\mu\text{m}$ , such models lead to predictions of  $\eta_{vitro}$  in good agreement with experimental data from glass tubes [21]. Blood flow in larger microvessels is more difficult to model, since cells do not usually flow in single file, and interactions between red cells must also be considered. Theoretical analyses of multi-file flow have been reviewed by Secomb [22].

### 3.4. Flow resistance in vivo

Direct measurement of blood viscosity in living microvessels is very difficult: this requires the simultaneous measurement of the pressure drop along a vascular segment, the volume flow in that segment and the length and inner diameter of the segment to calculate its hydraulic resistance. The calculation of apparent viscosity is especially sensitive to errors in the determination of vessel internal diameter. Lipowsky et al. [23,24] estimated in vivo blood viscosity in single unbranched microvessels ranging

in diameter from 7 to 60  $\mu\text{m}$  using a double micropipette measurement of pressure drop and the optical dual window method for determination of center-line flow velocity. They reported relative viscosity values of  $4.22 \pm 2.35$  ( $H_{s,y,s}$  0.36) and  $2.09 \pm 0.33$  ( $H_D \sim 0.36$ ) which are substantially higher than the respective values determined in glass tubes at comparable hematocrit levels (Fig. 1).

In an alternative approach, Pries et al. [25] compared the distributions of flow velocities in networks predicted by a mathematical model with the observed values. The deviations were larger than expected based on known sources of measurement error, and were ascribed in part to inadequacies of the assumed rheological behavior of blood, particularly the relation between apparent viscosity, vessel diameter and hematocrit (viscosity law). A set of different viscosity laws was tested, and the one yielding predictions in best agreement with the experimental data was assumed to represent the closest approach to the in vivo behavior.

The resulting 'in vivo viscosity law' (Fig. 1) was given as

$$\eta_{\text{in vivo}} = \left[ 1 + (\eta_{0.45}^* - 1) \cdot \frac{(1 - H_D)^C - 1}{(1 - 0.45)^C - 1} \cdot \left( \frac{D}{D - 1.1} \right)^2 \right] \cdot \left( \frac{D}{D - 1.1} \right)^2 \quad (7)$$

with  $C$  according to Eq. (5) and

$$\eta_{0.45}^* = 6 \cdot e^{-0.085D} + 3.2 - 2.44 e^{-0.06D^{0.645}} \quad (8)$$

In agreement with the direct viscosity measurements, these results indicate that in vivo viscosity is much higher in microvessels with diameters ranging between 4  $\mu\text{m}$  and 30  $\mu\text{m}$  than in vitro viscosity obtained in tubes of the same diameter. In addition, viscosity is strongly hematocrit-dependent. The model simulations using the in vivo viscosity law yielded values for the total pressure drop across the microvascular network of  $53.7 \pm 14.8$  mmHg in agreement with results of direct pressure measurements ( $61.9 \pm 16.7$  mmHg): in contrast, only about half that pressure drop was obtained if the in vitro viscosity was used ( $23.8 \pm 6$  mmHg). These results are supported by findings of Sutton and Schmid-Schönbein in a dilated skeletal muscle preparation perfused with erythrocyte suspensions [26]. They report that relative apparent viscosities determined in this setup are similar to values obtained in rotational viscometers or in large glass tubes (diameter  $> 0.8$  mm).

The physical reasons for the observed differences in effective viscosity between glass tubes and living microvessels are not well understood. Possible factors have, however, been proposed [16,25]: (1) An interaction of the macromolecular layer on the endothelial surface with the flowing components of the blood. Using data from a study of Born and Palinski [27] on the concentration of sialic acids on the surface of vascular endothelia, Silberberg [28]

calculated the thickness of the glycocalyx layer attached to the endothelial surface as 0.5  $\mu\text{m}$ . This concept corresponds to the 'retarded plasma layer' concept put forward by Desjardins and Duling [29,30] to explain low capillary tube hematocrits (see below). It was supported by recent observations of Reinhardt et al. [31] demonstrating the importance of the surface properties for the velocity of beads covered with endothelial cells falling in a suspension medium. (2) The effect of dimensional irregularities of vessel diameter [22,32] and of (3) vascular bifurcations both leading to additional energy dissipation due to rearrangement and shape changes of moving cells. (4) Additional pressure drop due to leukocyte traffic and plugging [33,34].

It is not known whether and how much the factors described above contribute to the observed discrepancy between in vitro and in vivo estimates of the apparent viscosity of blood. In a recent theoretical study, Wang and Parker [35] have considered the effect of a macromolecular layer, capable of retarding plasma flow, on particle motion in narrow tubes. Secomb and Hsu [36] have modeled the single-file motion of red blood cells through vessels with irregular cross-sections. These studies have shown that the hypothesized mechanisms may, at least in principle, lead to substantial increases in flow resistance above that in uniform glass tubes.

### 3.5. Aggregation and sedimentation

In normal blood, red blood cells tend to form aggregates resembling stacks of coins ('rouleaux'). The mechanism of this aggregation is not entirely understood, and two theories have been developed: (a) macromolecular bridging by proteins adsorbed onto the membrane surface of adjacent cells, and (b) osmotic water exclusion from the gap between two neighbouring red cell membranes. Red cell aggregation is a reversible phenomenon and aggregates can be easily disrupted by mechanical forces [37]. Therefore, the quantity and size of aggregates in the blood is a function of the balance between physicochemical binding forces and disrupting shear forces [9].

Aggregation is substantially intensified when the concentration of characteristic protein fractions is increased, most notably fibrinogen and alpha-2-macroglobulin. Under such conditions more complex three-dimensional aggregates are formed, including clumps of irregular shape and considerable size. The suspension stability of the blood is then severely reduced, with spontaneous phase separation occurring due to sedimentation of red cell aggregates in the gravitational field. Even with normal aggregation tendency, the formation of rouleaux is associated with mild phase separation because of the density difference between red cells and the plasma. At a given density difference, sedimentation velocity depends mainly on plasma viscosity and particle size. This is the basis of the clinical determination of sedimentation rate which is interpreted to qualita-

tively reflect changes of concentration and composition of the plasma proteins [14].

### 3.6. Occurrence of aggregation in the circulation

Red cell aggregation occurs in microcirculatory vessels even under perfectly healthy conditions. The degree to which aggregates are formed in flowing blood with a given plasma protein composition depends on the magnitude of shear forces prevailing and geometric constraints resulting from blood vessel dimensions [2]. Usually, the pronounced shear-sensitivity of aggregation prevents its occurrence in the high-shear flow regime in arterial vessels, and the narrow dimensions of blood capillaries do not allow red cell aggregates to develop. Thus, rouleaux formation is most often observed in post-capillary venules and smaller veins in which flow is relatively slow and shear forces do not suffice to cause aggregate disruption. The phenomenon is more apparent whenever the driving head of pressure is reduced or flow in postcapillary vessels is slowed down due to e.g. constriction of pre-capillary arterioles. It is, obviously, also more apparent in disease states in which the plasma protein composition has changed, such as in acute inflammation (so-called acute phase reactions) or, particularly, in clinical situations conditions involving the production of pathologic proteins of very high molecular weight.

Intensified red cell aggregation often associated with sluggish flow under conditions of disease has been interpreted to indicate a pronounced impairment of blood flow. This has led to the concept of 'sludged blood' as a major pathophysiological mechanism contributing to insufficient perfusion and thus delivery of substrates to peripheral tissues [38]. In support of this concept, intravascular sedimentation of red cell aggregates — a major component of the 'sludge' observed — was also seen. However, the microrheologic effects of aggregation per se and its combination with sedimentation on flow in narrow vessels have only recently been detailed by *in vitro* studies described below. Quantitative information on the consequences of aggregate formation in a complex network of microvessels *in vivo* is scarce. The results of whole organ studies either do not show much of an effect on overall flow resistance or are difficult to interpret because of methodological reasons: usually, aggregation is induced in these studies by adding high molecular weight colloids (mostly dextrans) to the blood. Since this also alters plasma viscosity and colloid osmotic pressure, the effects observed cannot only be interpreted as resulting from aggregation per se.

### 3.7. Aggregation and sedimentation during steady state tube flow

Several studies of the effect of aggregate formation on the characteristics of blood flow have been conducted in appropriately sized glass tubes. It is well established that enhanced aggregation causes an alteration of the cross-sectional

distribution of hematocrit, with the extent of marginal cell depletion and axial cell accumulation increasing with aggregation tendency [4,39]. It has also been shown that the widened cell-free lubrication layer at the vessel wall is associated with a reduction of the resistance to flow. By contrast, the axial cell core is condensed and travels as a plug with a practically flat velocity profile. This is also expressed by the enhancement of the Fahraeus effect: tube hematocrit decreases relative to discharge hematocrit. Since aggregation is shear-dependent, both the Fahraeus and the Fahraeus-Lindqvist effects increase with decreasing shear forces [40–43]. The extent of this shear-dependence depends on the size of the perfused tube: the effect of aggregation vanishes as tube diameter approaches that of small capillaries allowing only single file flow.

This description applies to flow in vertical tubes in which sedimentation of cells or aggregates occurs only in axial direction and therefore does not interfere with the cross-sectional cell distribution. However, sedimentation in radial direction, such as occurs in horizontal flow, causes the development of non-symmetric cross-sectional cell distribution. This is associated with a substantial elevation of resistance to flow because of the disappearance of a lubrication layer in the bottom part of the tube [44–46]. As a result, all rheologically relevant parameters are non-symmetrically distributed across the tube, with the distribution profiles differing in vertical and horizontal planes. For example, the velocity profiles may exhibit a pronounced overvelocity in the upper regions of the supernatant plasma zone, while a blunt profile exists in the sedimented red cell mass at the bottom [47]. In this situation, most of the white cells and platelets are observed in the red cell depleted upper flow regions. Consequently, the Fahraeus effect and thus local concentration in the tube of the different blood cell species may be quite different [48].

### 3.8. Time-dependence of blood rheology in tube flow

Red cell aggregation and sedimentation are time-dependent phenomena. Due to their influence on flow behavior of blood, the resistance to blood flow under constant hemodynamic conditions is substantially time-dependent. This is very relevant for the extrapolation of data obtained *in vitro*, i.e. in long straight tubes, to microvessels *in vivo*, since the transit time in every single segment of a microvascular network may be short compared to the characteristic times of the aggregation and sedimentation processes.

When changes of shear stress are acutely induced during tube flow of blood with normal aggregation tendency, several minutes are required before steady state flow is developed and the direction of the changes observed depends strongly on the extent of aggregation and the development of flow asymmetries due to sedimentation [43,47]. Therefore the effects of these phenomena in horizontal tubes differ from those in vertical tubes (Fig. 2). In the

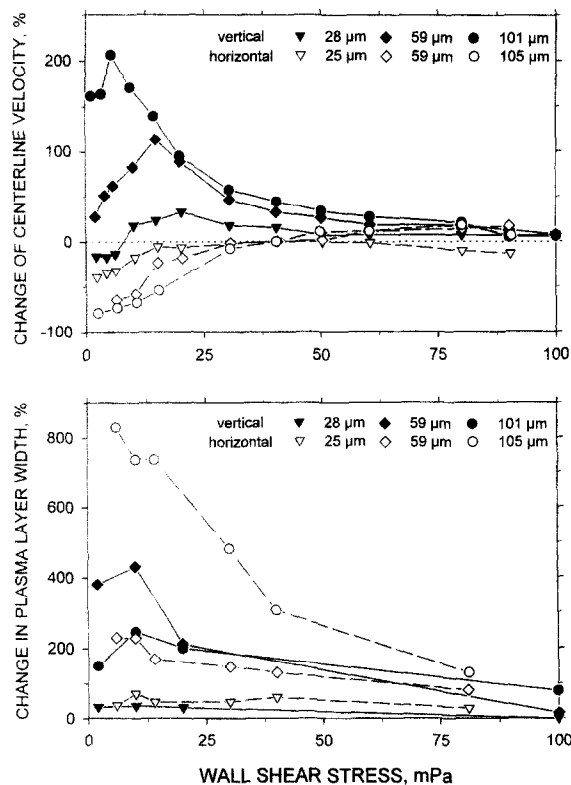


Fig. 2. Percentage changes of velocity (top) and cell deficient marginal plasma layer (bottom) over a 5 min observation time following a sudden reduction of shear stress from very high values. Measurements during flow of normal human blood through horizontal (open symbols) and vertical (closed symbols) tubes of different diameter. (Adapted from Alonso et al. [43,45]). It is clear that even with similar marginal plasma layer width, the time-dependent change of resistance is very different in the presence or absence of sedimentation.

latter, a sudden transition from high-shear flow of monodispersed red cells to low-shear flow with developing assembly of single cells to aggregates leads to a notably time-dependent decrease of effective viscosity due to the time-dependent depletion of red cells from the marginal flow regions and their incorporation into the axial cell core. This process starts within a few seconds and takes minutes to reach a steady state. In this sense, red cell aggregation facilitates blood flow, as already suspected by Fahraeus [49]. If the same experiment is made in horizontal tubes, the initial viscosity decrease is rapidly reversed and followed by a substantial increase above the control value. This represents the effect of aggregate sedimentation. The sequence of events observed thus shows that the effect of red cell aggregation on apparent viscosity precedes that of sedimentation, as might be expected, but the effective flow behavior in horizontal flow is eventually completely dominated by the developing flow asymmetry (Fig. 2).

### 3.9. Theory of aggregation and sedimentation in microvessels

The 'stacked-coins model' mentioned previously is applicable to the motion of an aggregated core, approximated

as a rigid cylindrical plug, along the center-line of a vessel. The increase in width of the cell-free layer resulting from aggregation may be expressed as a decrease in  $\lambda$  [Eq. (6)], with a resulting decrease in viscosity ( $\eta_{\text{vitro}}$ ). Cokelet and Goldsmith [42] refined this basic model to include effects of relative motion within the core and sedimentation parallel to the tube axis. Murata and Secomb [50] modeled the transition from a fully aggregated core to freely suspended cells with increasing flow rate. Effects of sedimentation in non-vertical tubes have been analyzed by Secomb and El-Kareh [51], assuming that the core remains cylindrical and fully aggregated. The predictions of these models are generally consistent with observed behavior. However, the observed dependence of sedimentation on flow rate has not been successfully modeled to date. Also, the effects of progressive sedimentation along the length of a vessel are not well understood. Further work is required to develop quantitative understanding of this behavior, and its significance for in vivo blood flow.

## 4. Blood flow in networks

### 4.1. Phase separation at microvascular bifurcations

At diverging branch points of the microvasculature, the blood flow in a parent vessel is divided as it enters two daughter vessels. Blood is a two-phase fluid (red cells and plasma) and these components may be distributed non-proportionally between the daughter vessels, one receiving a higher hematocrit than that of the parent vessel, and the other receiving a lower hematocrit. This phenomenon was observed early in the development of intravital microscopy. Krogh coined the term 'plasma skimming' to describe the observation that a smaller side branch of an arteriole may 'skim' the cell-poor marginal fluid layers of its feeding vessel. Such behavior reflects axial migration of red cells upstream of the bifurcation, producing a phase separation in the parent vessel. At the bifurcation, fluid streams carrying blood of different hematocrits enter the two daughter vessels.

Phase separation can, however, also be effected by the fluid forces directly at a bifurcation: since blood cells are particles of finite size, a certain fraction of them will always be found travelling along the dividing stream surface which — in the absence of cells — would separate the flow compartments entering the respective daughter vessels. Only at the branch point will the balance of fluid forces decide which way such cells are to go, thereby leading to a partial separation of solid and fluid phase. This process, which does not require an uneven distribution of hematocrit in the parent vessel, has been named 'red cell screening' [52] and will be relevant to an increasing relative number of cells as the particle to tube diameter ratio increases.

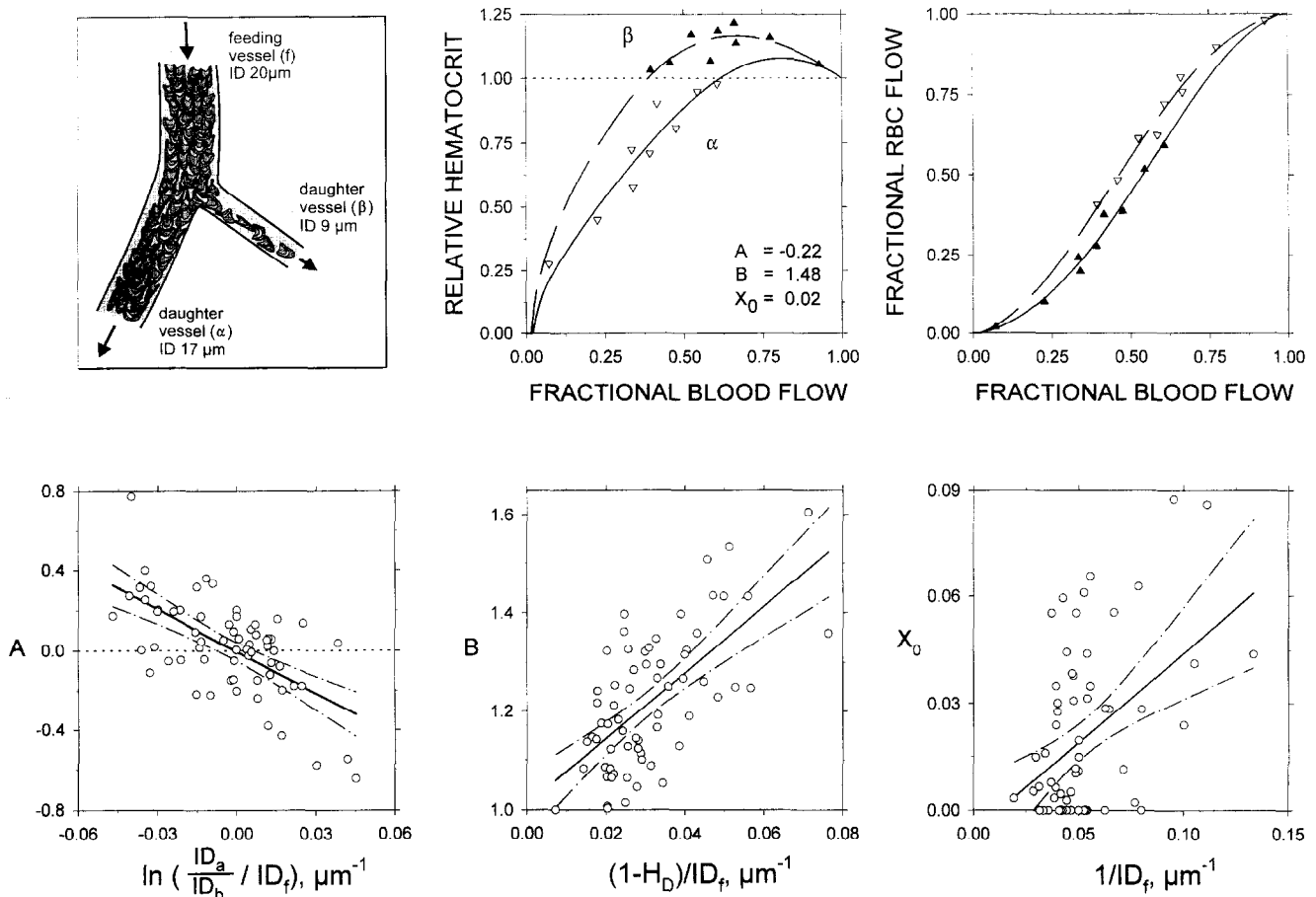


Fig. 3. Phase separation. *Upper*: Schematic drawing of a microvascular bifurcation (*left*). Hematocrit relative to that in the feeding vessel (*middle*) and fractional erythrocyte flow (*right*) in both daughter branches versus the fractional blood flow in that branch. The symbols depict results of experimental measurements while the continuous lines and the parameters given correspond to the logit fit of the data obtained with Eq. (9). *Lower*: Parameters of the logit fit ( $A$ ,  $B$ ,  $X_0$ ) obtained for 65 bifurcations in the mesentery plotted versus the relevant combinations of independent variables. The respective linear regression lines ( $A = -6.96 \ln(D_a/D_b)/D_f$ ;  $B = 1 + 6.98(1 - H_D)/D_f$ ;  $X_0 = 0.4/D_f$ ;  $D_a$ ,  $D_b$ ,  $D_f$  are the diameters of the two daughter branches and the feeding vessel) are shown with their 95% confidence intervals (Adapted from Pries et al. [71]).

#### 4.2. Experimental studies of phase separation

Since measurements and manipulation of the pertinent parameters in vivo is very difficult, a number of in vitro approaches has been used to characterize phase separation effects and their dependence on morphological and hydrodynamical conditions at a branch point [53–65]. However, phase separation has also been characterized and quantified in vivo [66–71] leading to qualitatively similar results.

In these studies a number of factors influencing phase separation has been identified. Among these, the most basic one is the flow split at the bifurcation quantified by the fraction of blood flow in the feeding vessel being diverted into a given daughter branch: the daughter branch with the lower fractional blood flow ( $FQ_B$ ) in most cases exhibits a reduced hematocrit while the other branch carries blood of a hematocrit above that in the mother vessel.

To characterize the phase separation properties of bifurcations, the hematocrit in a daughter branch divided by that in the mother vessel or the fractional erythrocyte flow into that branch ( $FQ_E$ ) have been plotted versus its frac-

tional blood flow [60,65,68,69,72] (Fig. 3). In the latter plot, all data fall on the line of identity in the absence of phase separation. The deviation of experimental data from this line can be empirically separated into three categories: (1) For  $FQ_B$  values below a certain **threshold**, a daughter branch may carry only cell-free plasma. (2) In the  $FQ_B$  range above that threshold the  $FQ_E$  versus  $FQ_B$  relation may exhibit a variable degree of non-linearity leading to a **sigmoidal shape** of the curve. (3) The  $FQ_E$  values for both daughter branches may differ for corresponding values of fractional blood flow ( $FQ_B$ ). In this case, the  $FQ_E$  versus  $FQ_B$  relations for each daughter branch are **asymmetric** with respect to the point  $FQ_E = FQ_B = 0.5$ .

Based on experiments at 65 bifurcations in the rat mesentery, Pries et al. [71] proposed a parametric description of phase separation in vivo. Using a logit function to describe the dependence of  $FQ_E$  on  $FQ_B$  for each bifurcation,

$$FQ_E = \frac{1}{1 + e^{-\left(A + B \logit\left(\frac{FQ_B - X_0}{1 - 2X_0}\right)\right)}} \quad (9)$$

threshold, asymmetry and sigmoidal shape were quantified by the parameters  $X_0$ ,  $A$ , and  $B$  (Fig. 3).

For the set of bifurcations analyzed, these parameters were correlated with factors possibly determining phase separation properties of a given bifurcation. Among those factors, the size of the bifurcation, the relative size of the daughter branches and the hematocrit level and profile in the feeding vessel turned out to be most important. In very different experimental situations *in vitro* and *in vivo* the extent of phase separation increases with decreasing size of the vessel feeding the branch point and decreasing hematocrit (Fig. 3) [57,60,62,65,68,71]. In addition it was shown that phase separation increases with the size difference between the daughter branches [60,65,71]. For equal flow split, this leads to a higher hematocrit in the smaller side branch.

#### 4.3. Theoretical models of phase separation

While parametric descriptions according to Eq. (9) represent useful tools for mathematic modelling of blood flow through microvascular networks, the available experimental data present a large degree of scatter which can only in part be attributed to the independent variables measured in the experiments (size of the vessels joined at the bifurcation and hematocrit in the feeding vessel). This could in part be due to relevant variables not included in the quantitative analysis like, e.g., asymmetric shapes of the hematocrit profiles in the feeding vessels [60,61].

Detailed theoretical analysis could help to improve the descriptions of phase separation phenomena by pointing out potentially relevant factors which have not been adequately represented in experimental studies. Most mathematical models of phase separation presented in the past restrict themselves to the unproportional distribution of red cells and plasma (or the suspending medium) by pure plasma skimming, and hematocrit is treated as a continuous local property of the fluid. These restrictions given, the system can be completely described by the radial hematocrit and velocity profile in the feeding vessel plus the shape of the stream surface separating the fluid domains entering the respective daughter vessels. Such models have been used to derive predictions or fits for the relationship between  $FQ_E$  and  $FQ_B$  [59–62,64,65,73,74] or to predict the shape of the hematocrit profile in the feeding vessel from measurements of fractional red cell and blood flow [52,71].

A fundamental restriction of plasma skimming models is the neglect of phenomena resulting from the finite size of red cells. As stated above, phase separation increases with decreasing vessel diameter and is especially important for vessel diameters well below 30  $\mu\text{m}$ . In this diameter range, the cell to tube diameter ratio ( $\lambda$ ) cannot realistically be assumed to be zero, and red cell trajectories may significantly depart from fluid streamlines. Using a two-dimensional analogue of the bifurcation geometry, Audet

and Olbricht [75] calculated trajectories of rigid particles with  $\lambda$  values ranging from 0.2 to 0.8 flowing at different radial positions in the feeding channel. The results show that even for the modelled conditions of low Reynolds number flow where inertial forces play a negligible role, particles do not always follow the fluid streamline in which their center is located, leading to red cell screening at the bifurcation.

#### 4.4. Network architecture and flow

The distributions of blood flow and red cell flux in a microvascular network depend on the network architecture, the resistance to flow in each segment, and the partition of red cells in diverging bifurcations. It is obvious from both anatomical studies and intravital microscopy that microvascular networks exhibit highly asymmetric and heterogeneous architecture. Consequently, hemodynamic variables, such as blood flow velocity and hematocrit, are highly variable within a network, even among morphologically similar vessels. This variability complicates quantitative analyses of network hemodynamics and results in a behavior that is qualitatively different from what would be found in highly symmetric networks. Examples of this behavior are discussed below.

Blood flowing through a microvascular network generally passes through vessels of successively decreasing diameter, until the capillaries are reached, and then again through vessels with increasing diameters on the venous side. For this reason, experimental measurements of hemodynamic parameters within networks have often been represented as functions of vessel diameter, distinguishing between arteriolar and venular vessels. Several basic aspects of network hemodynamics are evident in such studies [76–78]. Blood flow velocity is positively correlated with vessel diameter in both arterioles and venules. Higher velocities are present in arterioles than in venules with the same diameter. This implies that wall shear rates, and hence pressure gradients, are generally higher on the arteriolar side. Most of the pressure drop in the microcirculation occurs in small arterioles ( $D < 40 \mu\text{m}$ ), which are the principal site of active diameter changes to achieve regulation of blood flow. Mean capillary pressure is therefore much closer to venous pressure than to arterial pressure. The resulting low capillary pressure level is relevant for the maintenance of tissue fluid balance.

#### 4.5. Consequences of heterogeneity

As already stated, network architecture and hemodynamics exhibit a high degree of heterogeneity. This heterogeneity cannot be treated simply as a phenomenon of biological randomness, but must be regarded as an intrinsic functional property of microvascular networks. Estimates of mean parameters do not provide a sufficient basis for quantitative analyses of network functions; their distribu-

tions must also be considered, since estimates of the derived quantity based on solely mean values of the underlying parameters may be seriously in error [79–81]. Such errors can arise in two main cases, which are not mutually exclusive: (i) when a derived quantity depends nonlinearly on one or more underlying parameters; or (ii) when the derived quantity depends on two or more underlying parameters which are themselves statistically correlated.

As an example of case (i), blood flow through a vessel is nonlinearly related to vessel diameter, and so an estimate based on mean diameter may be in error. Similarly, solute clearance in a vascular segment or bed is nonlinearly dependent on its permeability–surface area product and the plasma flow [82], and so its estimate requires consideration of the distributions of these variables.

Multiple correlations exist among hemodynamic parameters in microvascular networks, leading to case (ii) above. Such correlations influence extrapolations from microvascular measurements to whole-organ behavior [83], and their neglect can contribute to the apparent discrepancy between such extrapolations and direct whole-organ measurements [84]. For example [81], if the transit time of blood through microvascular networks of the rat mesentery was calculated from average values of flow velocity and vessel segment length measured in single vessels, a value of 6.5 s was obtained. This value was about 60% higher than the true mean value (4.08 s) determined by an analysis of flow distribution in networks of this tissue. Further examples of the effect of correlations involving segment hematocrits on mean network properties are described next.

#### 4.6. Network Fahraeus effect

Unequal partition of hematocrit at successive arteriolar branch points leads to a high degree of heterogeneity in the hematocrit of individual segments. Furthermore, the tendency of red cells to follow the higher-flow pathway at each bifurcation results in a strong correlation between hematocrit and flow velocity. Such a correlation (vessels which exhibit higher flow velocities on average also exhibit higher hematocrits) causes a reduction of average capillary discharge hematocrit ( $\bar{H}_D$ ) compared to the hematocrit of blood flowing through the feed arteriole ( $H_D^*$ ). This effect is analogous to the reduction of hematocrit within a single segment (the Fahraeus effect) which results from the correlation between hematocrit and velocity within a single vessel cross-section. For this reason, the reduction of average capillary discharge hematocrit has been called the network Fahraeus effect [85].

Due to the network Fahraeus effect and the correlation between diameter and hematocrit, the  $\bar{H}_D$  on the capillary level in the rat mesentery is reduced relative to  $H_D^*$  by about 20% [19,81]. Using flow modelling in computer-generated asymmetric vessel networks, Levin et al. [86] found that this hematocrit reduction varies strongly in

response to the phase separation characteristics used in the model. With increasing extent of phase separation, maximum reductions of about 40% were reached. These findings can have physiological implications since phase separation characteristics may change with the composition of the blood, the aggregation tendency, and hematocrit. For example, the hematocrit reduction by isovolemic hemodilution leads to increased phase separation and therefore to an increased network Fahraeus effect. In the rat mesentery a reduction of the systemic hematocrit ( $H_{sys}$ ) from 47% to 32% led to a decrease of the quotient  $\bar{H}_D/H_{sys}$  from about 0.78 to 0.65 [19].

#### 4.7. Microvascular hematocrit levels

While it could be shown for complete data sets on microvascular networks in the rat mesentery that the observed reduction of both tube and discharge hematocrit can be sufficiently explained by the above-mentioned effects, it is still not clear whether additional phenomena are present in tissues where especially low capillary hematocrits ( $H_T$ ) have been measured [87,88]. The existence of a plasma layer adjacent to the vessel wall in muscle capillaries has been proposed [29,30,89] in which the flow is restricted due to the macromolecules residing at the endothelial surface (see discussion in Section 3.4). Such a ‘retarded (or stagnant) plasma layer’ would decrease the measured tube hematocrit for a given  $H_D$  and thereby add to the reduction of average capillary  $H_T$ .

The retarded layer concept was supported by experiments in which microperfusion of capillaries with heparinase led to an increase in  $H_T$  [30]. This result was interpreted to indicate that the macromolecular wall layer is digested by heparinase leading to an increase of the effective vessel diameter. It was also suggested that the thickness of the macromolecular layer could vary inversely with the blood flow velocity. Such a mechanism would lead to a decrease of geometrical hindrance with increasing pressure head especially in the capillary bed, thereby increasing the impact of adjustments in arteriolar diameter on microvascular perfusion. In addition, a reduction of stagnant layer thickness with increasing flow velocity would decrease the diffusion distance for  $O_2$  and  $CO_2$  in high perfusion states. However, direct evidence for the existence of a wall adjacent layer with restricted flow of sufficient thickness to explain the observed effects on  $H_T$  (about 0.5  $\mu\text{m}$ ) is still missing.

#### 4.8. Pathway effect and tissue Fahraeus effect

Phase separation not only generates a positive correlation between velocity and hematocrit but also influences the distribution of red cell flow and hematocrit to capillaries of different generations. If a main arteriole feeding a microvessel network gives rise to smaller side branches, these vessels will mostly exhibit hematocrit values below

that of their feeding vessel. This, in turn, leads to a small increase of hematocrit in the main arteriole. Since this phenomenon is repeated at up to 25 consecutive arteriolar branch points in a microvascular network, it leads to a substantial build-up of hematocrit with increasing generation level along the arteriolar vessel tree and therefore also in the capillaries fed by it. This phenomenon increases the probability for red cells to travel on long flow pathways through microvascular networks and has been termed 'pathway effect' [19,90].

Together with the vessel Fahraeus effect, the network Fahraeus effect and the pathway effect determine the relation between the hematocrit of the blood contained in the vessels of a microvascular network ( $\bar{H}_D^V$ , volume-weighted mean of tube hematocrit for all vessels contained in a given vascular bed) and the hematocrit fed into it ( $H_D^*$ ). The reduction of  $\bar{H}_D^V$  with respect to  $H_D^*$  has been called tissue Fahraeus effect [90]. The quotient  $\bar{H}_D^V/H_D^*$  is identical to that of the average transit time of red cells through the tissue ( $\bar{t}_c$ ) divided by the average transit time of blood ( $\bar{t}_b$ ), which can be expressed in terms of the average transit times of cells, and plasma,  $\bar{t}_p$ ) [90,91],

$$TF = \frac{\bar{H}_D^V}{H_D^*} = \frac{\bar{t}_c}{\bar{t}_b} = \frac{\bar{t}_c}{\bar{t}_c \cdot H_D + \bar{t}_p \cdot (1 - H_D)} \quad (10)$$

This equation allows the comparison of results from measurements of cell and plasma transit times with hematocrit determinations either by indicator dilution methods or by direct intravital observation. Lipowsky et al. [91] report values of 0.79 for  $TF$  for the cat mesentery and of 0.82 for the rat cremaster. From hematocrit determinations in all segments of six microvascular networks in the rat mesentery, we derived a  $TF$  value of  $0.79 \pm 0.02$ . Indicator dilution studies [92] where the average hematocrit was determined for a number of different tissues and organs yield  $TF$  values between 1.5 and 2 in the spleen down to less than 0.5 for the gut and the testis. These tissue and organ differences indicate that the extent to which vessel and network Fahraeus effect and pathway effect influence average tissue hematocrit differs drastically probably due to differences in angioarchitecture.

#### 4.9. Theoretical models of network hemodynamics

Theoretical models have played an important part in efforts to gain a quantitative understanding of network hemodynamics. They permit systematic exploration of the relationships between network architecture, the rheological behavior of the blood, and the resulting patterns of blood flow and hematocrit distribution. Their development has been reviewed by Popel [93]. Most such simulations have used the same basic approach [16,25,94,95]. The network is described as an assemblage of segments and nodes

(bifurcations), with specified topology and segment vessels and diameters. The resistance of each segment is estimated, and the flow in each is expressed in terms of the nodal pressures. A system of linear equations involving the pressures is obtained by applying the condition that the flows entering or leaving each node must sum to zero. This is solved for the pressures and the flows, and the distribution of hematocrit is obtained using information on the partition of hematocrit at bifurcations. The initial estimates of segment resistance are then updated, based on the hematocrit values, and the procedure is repeated iteratively until convergence is achieved. One variation is to track the motion of individual red cells through the network [32,68].

This approach has been used to examine many aspects of network hemodynamics. Lipowsky and Zweifach [94] and Fenton and Zweifach [95] computed distributions of intravascular pressures with vessel diameter and compared the results with experimental data. The contribution of white cells to network hemodynamics was examined by Fenton et al. [96] and Warnke and Skalak [97]. Pries et al. [16,25] used this approach to deduce the *in vivo* variation of apparent blood viscosity with vessel diameter, as mentioned earlier.

Dawant et al. [98] and Levin et al. [86] examined the effects of network heterogeneity on the distributions of pressure, flow and hematocrit. A further study was made by Pries et al. [99]. In these studies, two components of network heterogeneity were identified: 'geometrical', i.e. dispersion in segment lengths and diameters, and topological, i.e., asymmetries in network topology. The study of Pries et al. [99], which was based on the observed architecture of a network in the rat mesentery, indicated that the distribution of pressure in the network, its overall resistance to flow, and the pathway effect are mainly dependent on the network's topological heterogeneity, while mean capillary hematocrit (network Fahraeus effect) was more sensitive to geometrical heterogeneity. Both topological and geometric heterogeneity contributed substantially to the predicted dispersion in the transit time of blood through the network.

#### 4.10. Hydrodynamic factors in the design of vascular networks

Vascular systems have to adapt continually to changing functional needs and to maintain an angioarchitecture which creates adequate hemodynamic conditions. Murray [100] developed a hypothesis stating that the vasculature is designed such that operating 'costs' of the circulatory system are minimized. This led to the conclusion that volume flow is proportional to vessel diameter cubed ( $D^3$ ), and shear stress at the vessel wall is uniform throughout the network. A vascular response to local shear rate at the endothelial surface was assumed to provide the

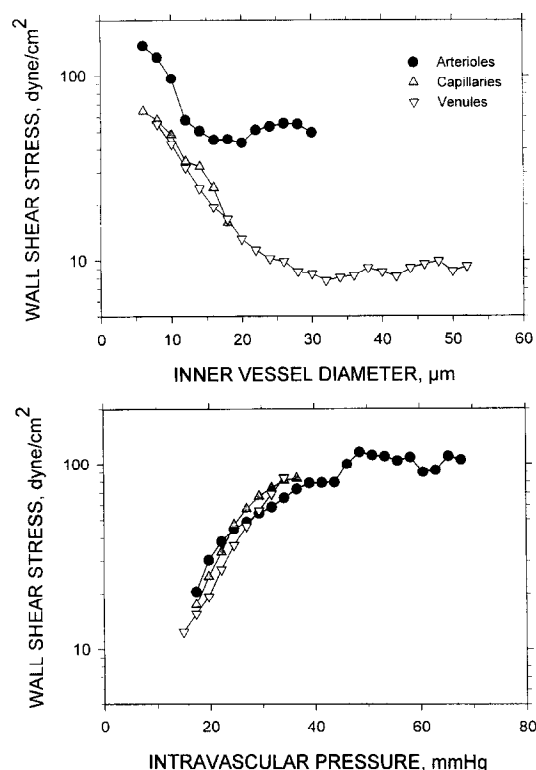


Fig. 4. Wall shear stress in vessel segments of 6 networks of the rat mesentery as a function of vessel diameter (upper panel) and intravascular pressure (lower panel) for arterioles, capillaries, and venules (modified after Pries et al. [105]). Wall shear stress and pressure were predicted by mathematical flow simulation [25].

basis of vascular adaptation needed to maintain constant shear rates [101]. Constant shear rates were demonstrated for the arterial tree down to small arterioles [102], but shear rates in larger venules differ from those in arterioles, and in precapillary and capillary vessels an increase of shear stress (or shear rate) with decreasing vessel diameter is observed (Fig. 4).

It is known that vessels respond not only to shear rate but also to the distending transmural pressure [103] suggesting a role of pressure in the control of vascular structure and network hemodynamics [104]. Data obtained in complete microvascular networks showed a strong, unified dependence of shear rate and shear stress on pressure for arterioles, capillaries and venules (Fig. 4) [81,105]. From these data a pressure–shear hypothesis for the control of vascular design was derived: vascular beds grow and adapt so as to maintain the shear stress in each vessel at a level which depends on local transmural pressure [105]. According to this hypothesis, the local vascular responses to intravascular pressure *and* to shear stress at the endothelial surface work to enforce a general design principle of vascular systems under both normal and pathological conditions (such as hypertension). In contrast to Murray's minimum-cost concept, the pressure–shear hypothesis provides an explanation for the physiologically vital arterio-

venous asymmetry of vascular beds with low capillary pressures.

## 5. Conclusions and future directions

The biophysics of blood flow in the microvasculature involves an intricate interaction between the mechanical behavior of blood and its cellular constituents, and the complex and irregular geometries of networks of microvessels. Studies extending over most of the present century have led to basic understanding in several areas, including the following points:

- Mammalian red blood cells are highly deformable, and this enables them to pass through narrow capillaries. Furthermore, they are typically surrounded by a layer of reduced or zero hematocrit when flowing through microvessels. This cell-poor layer strongly influences the rheological behavior of blood in microvessels, and can be modified by intravascular aggregation and sedimentation of red blood cells.
- The apparent viscosity of blood flowing through narrow glass tubes decreases with decreasing tube diameter, down to less than 10  $\mu\text{m}$ . However, the resistance to flow in microvessels *in vivo* is substantially higher than that in glass tubes with corresponding diameters.
- Functional properties of microvascular networks depend not only on their mean properties, but on the heterogeneity of their architecture. For example, mean capillary hematocrit and the overall resistance to blood flow are dependent on the heterogeneity of network geometry and topology.

However, a number of unresolved issues remain, particularly with regard to the relationship between blood flow properties as observed *in vitro* and the functional behavior of blood in the living microcirculation. Future studies should address these issues, including the following:

- The causes of the discrepancy between the apparent viscosity of blood in microvessels *in vivo* and that in glass tubes have not been established.
- The *in vivo* significance of red cell aggregation and sedimentation in both normal and pathological situations continues to be subject to debate.
- Although measurements of the bulk viscosity of blood and red cell deformability are frequently correlated with specific clinical conditions, the actual significance of such measures with regard to blood circulation is poorly understood.
- The mechanics of red cell screening in microvascular bifurcations is not well understood, although this phenomenon is probably very significant in smaller bifurcations.
- The high level of heterogeneity in microvascular hemodynamics is recognized, but efforts to understand its implications for the mass transport functions of the microcirculation are at a relatively early stage.

## References

- [1] Gaehtgens P. Hemodynamics of the microcirculation. Physical characteristics of blood flow in the microvasculature. In: Meesen H, ed. *Handbuch der allg. Pathologie III/7 Mikrozirkulation*. Berlin, Heidelberg: Springer, 1977:231–87.
- [2] Chien S, Usami S, Skalak R. Blood flow in small tubes. In: Renkin EM, Michel CC, Geiger SR, eds. *Handbook of Physiology: The Cardiovascular System IV*. Chapter 6. Bethesda, MD: American Physiological Society, 1984:217–49.
- [3] Zweifach BW, Lipowsky HH. Pressure–flow relations in blood and lymph microcirculation. In: Renkin EM, Michel CC, eds. *Handbook of Physiology, Section 2: The Cardiovascular System Vol. IV. Microcirculation Part 1*. Chapter 7. Bethesda, MD: American Physiological Society, 1984:251–307.
- [4] Goldsmith HL, Cokelet GR, Gaehtgens P, Robin Fahraeus: evolution of his concepts in cardiovascular physiology. *Am J Physiol* 1989;257:H1005–15.
- [5] Secomb TW. Red blood cell mechanics and capillary blood rheology. *Cell Biophys* 1991;18:231–51.
- [6] Skalak R. Rheology of red blood cell membrane. In: Grayson J, Zingg W, eds. *Microcirculation*. Vol. I. New York: Plenum Press, 1976:53–70.
- [7] Hochmuth RM, Waugh RE. Erythrocyte membrane elasticity and viscosity. *Annu Rev Physiol* 1987;49:209–19.
- [8] Evans EA, Hochmuth RM. Membrane viscoelasticity. *Biophys J* 1976;16:1–11.
- [9] Chien S. Biophysical behavior of red cells in suspensions. In: Surgenor DM, ed. *The Red Blood Cell*. Vol. II. 2nd edition. New York: Academic Press, 1975:1031–133.
- [10] Schmid-Schönbein GW, Sung KP, Tözeren H, Skalak R, Chien S. Passive mechanical properties of human leukocytes. *Biophys J* 1981;36:243–56.
- [11] Bayliss LE. The axial drift of the red cells when blood flows in a narrow tube. *J Physiol (Lond)* 1959;149:593–613.
- [12] Goldsmith HL, Mason SG. Axial migration of particles in Poiseuille flow. *Nature* 1961;190:1095–6.
- [13] Albrecht KH, Gaehtgens P, Pries A, Heuser M. The Fahraeus effect in narrow capillaries (i.d. 3.3 to 11.0  $\mu\text{m}$ ). *Microvasc Res* 1979;18:33–47.
- [14] Fahraeus R. The suspension stability of the blood. *Physiol Rev* 1929;9:241–74.
- [15] Barbee JH, Cokelet GR. The Fahraeus effect. *Microvasc Res* 1971;3:6–16.
- [16] Pries AR, Secomb TW, Gaehtgens P, Gross JF. Blood flow in microvascular networks — experiments and simulation. *Circ Res* 1990;67:826–34.
- [17] Martini P, Pierach A, Schreyer E. Die Strömung des Blutes in engen Gefäßen. Eine Abweichung vom Poiseuille'schen Gesetz. *Dtsch Arch Klin Med* 1930;169:212–22.
- [18] Fahraeus R, Lindqvist T. The viscosity of the blood in narrow capillary tubes. *Am J Physiol* 1931;96:562–8.
- [19] Pries AR, Fritzsche A, Ley K, Gaehtgens P. Redistribution of red blood cell flow in microcirculatory networks by hemodilution. *Circ Res* 1992;70:1113–21.
- [20] Whitmore RL. *Rheology of the Circulation*. Oxford: Pergamon Press, 1968.
- [21] Secomb TW. Flow-dependent rheological properties of blood in capillaries. *Microvasc Res* 1987;34:46–58.
- [22] Secomb TW. Mechanics of blood flow in the microcirculation. In: Ellington CP, Pedley TJ, eds. *Biological Fluid Dynamics*. Cambridge: Company of Biologists 1995, pp. 305–321.
- [23] Lipowsky HH, Kovalcheck S, Zweifach BW. The distribution of blood rheological parameters in the microcirculation of cat mesentery. *Circ Res* 1978;43:738–49.
- [24] Lipowsky HH, Usami S, Chien S. In vivo measurements of 'apparent viscosity' and microvessel hematocrit in the mesentery of the cat. *Microvasc Res* 1980;19:297–319.
- [25] Pries AR, Secomb TW, Geßner T, Sperandio MB, Gross JF, Gaehtgens P. Resistance to blood flow in microvessels in vivo. *Circ Res* 1994;75:904–15.
- [26] Sutton DW, Schmid-Schönbein GW. The pressure–flow relation in resting rat skeletal muscle perfused with pure erythrocyte suspensions. *Biorheology* 1995;32:29–42.
- [27] Born GVR, Palinski W. Unusually high concentrations of sialic acids on the surface of vascular endothelia. *Br J Exp Pathol* 1985;66:543–549.
- [28] Silberberg A. The physiological role of a thick gel-like layer over the endothelial surface. *Int J Microcirc Clin Exp* 1990;9(suppl 1):204(abstract).
- [29] Desjardins C, Duling BR. Microvessel hematocrit: measurement and implications for capillary oxygen transport. *Am J Physiol* 1987;252:H494–503.
- [30] Desjardins C, Duling BR. Heparinase treatment suggests a role for the endothelial cell glycocalyx in the regulation of capillary hematocrit. *Am J Physiol* 1990;258:H647–59.
- [31] Reinhart WH, Boulanger CM, Lüscher TF, Haeberli A, Straub PW. Influence of endothelial surface on flow velocity in vitro. *Am J Physiol* 1993;265:H523–9.
- [32] Kiani MF, Cokelet GR, Sævius IH. Effect of diameter variability along a microvessel segment on pressure drop. *Microvasc Res* 1993;45:219–32.
- [33] Braide M, Amundson B, Chien S, Bagge U. Quantitative studies on the influence of leukocytes on the vascular resistance in a skeletal muscle preparation. *Microvasc Res* 1984;27:331–52.
- [34] Warnke KC, Skalak TC. Leukocyte plugging in vivo in skeletal muscle arteriolar trees. *Am J Physiol* 1992;262:H1149–55.
- [35] Wang H, Parker KH. The effect of deformable porous surface layers on the motion of a sphere in a narrow cylindrical tube. *J Fluid Mech* 1995;283:287–305.
- [36] Secomb TW, Hsu R. Motion of red blood cells in capillaries with variable cross-sections. *J Biomech Eng* 1997; in press.
- [37] Schmid-Schönbein H, Gaehtgens P, Hirsch H. On the shear rate dependence of red cell aggregation in vitro. *J Clin Invest* 1968;47:1447–54.
- [38] Knisely MH. Intravascular erythrocyte aggregation (blood sludge). In: Hamilton WF, Dow P, eds. *Handbook of Physiology, Circulation Vol. III. Chapter 63*. Washington, DC: American Physiological Society, 1965:2249–92.
- [39] Palmer AA, Jedrzejczyk HJ. The influence of rouleaux on the resistance of flow through capillary channels at various shear rates. *Biorheology* 1975;12:265–70.
- [40] Gaehtgens P, Albrecht KH, Kreutz F. Fahraeus effect and cell screening during tube flow of human blood. I. Effect of variation of flow rate. *Biorheology* 1978;15:147–54.
- [41] Gaehtgens P, Kreutz F, Albrecht KH. Fahraeus effect and cell screening during tube flow of human blood. II. Effect of dextran-induced cell aggregation. *Biorheology* 1978;15:155–61.
- [42] Cokelet GR, Goldsmith HL. Decreased hydrodynamic resistance in the two-phase flow of blood through small vertical tubes at low flow rates. *Circ Res* 1991;68:1–17.
- [43] Alonso C, Pries AR, Gaehtgens P. Time-dependent rheological behaviour of blood at low shear in narrow vertical tubes. *Am J Physiol* 1993;265:H553–61.
- [44] Reinke W, Gaehtgens P, Johnson PC. Blood viscosity in small tubes: effect of shear rate, aggregation and sedimentation. *Am J Physiol* 1987;253:H540–7.
- [45] Alonso C, Pries AR, Gaehtgens P. Time-dependent rheological behaviour of blood flow at low shear in narrow horizontal tubes. *Biorheology* 1989;26:229–46.
- [46] Göbel W, Perkkio J, Schmid-Schönbein H. Compaction stasis due to gravitational red cell migration and floatational plasma skimming. *Virchow's Arch Allg Pathol Anat Histol* 1989;415:243–51.

- [47] Alonso C, Pries AR, Kießlich O, Lerche D, Gaetgens P. Transient rheological behaviour of blood in low-shear tube flow: velocity profiles and effective viscosity. *Am J Physiol* 1995;268:H25–32.
- [48] Schmid-Schönbein H. Fahraeus effect reversal in compaction stasis: microrheological and haemodynamic consequences of intravascular sedimentation of red cell aggregates. *Biorheology* 1988;25:355–66.
- [49] Fahraeus R. The influence of the rouleaux formation of the erythrocytes on the rheology of the blood. *Acta Med Scand* 1958;161:151–65.
- [50] Murata T, Secomb TW. Effects of aggregation on the flow properties of red blood cell suspensions in narrow vertical tubes. *Biorheology* 1989;26:247–59.
- [51] Secomb TW, El-Kareh AW. A model for motion and sedimentation of cylindrical red-cell aggregates during slow blood flow in narrow uniform tubes. *J Biomech Eng* 1994;116:243–9.
- [52] Pries AR, Albrecht KH, Gaetgens P. Model studies on phase separation at a capillary orifice. *Biorheology* 1981;18:355–67.
- [53] Bugliarello G, Hsiao GCC. Phase separation in suspensions flowing through bifurcations: a simplified hemodynamic model. *Science* 1964;143:469–71.
- [54] Cokelet GR. Macroscopic rheology and tube flow of human blood. In: Grayson J, Zingg W, eds. *Microcirculation*. Vol. 1. New York: Plenum Publ Corp, 1976:9–31.
- [55] Levine R, Goldsmith HL. Particle behaviour in flow through small bifurcations. *Microvasc Res* 1977;14:319–44.
- [56] Yen RT, Fung YC. Effect of velocity distribution on red cell distribution in capillary blood vessels. *Am J Physiol* 1978;235:H251–7.
- [57] Dellimore JW, Dunlop MJ, Canham PB. Ratio of cells and plasma in blood flowing past branches in small plastic channels. *Am J Physiol* 1983;244:H635–43.
- [58] Ofjord ES, Clausen G. Intrarenal flow of microspheres and red blood cells: skimming in slit and tube models. *Am J Physiol* 1983;245:H429–36.
- [59] Perkkio J, Keskinen R. Hematocrit reduction in bifurcations due to plasma skimming. *Bull Math Biol* 1983;45:41–50.
- [60] Fenton BM, Carr RT, Cokelet GR. Nonuniform red cell distribution in 20–100 micron bifurcations. *Microvasc Res* 1985;29:103–26.
- [61] Carr RT, Wickham LL. Plasma skimming in serial microvascular bifurcations. *Microvasc Res* 1990;40:179–90.
- [62] Carr RT, Wickham LL. Influence of vessel diameter on red cell distribution at microvascular bifurcations. *Microvasc Res* 1991;41:184–96.
- [63] Rong FW, Carr RT. Dye studies on flow through branching tubes. *Microvasc Res* 1990;39:186–202.
- [64] Enden G, Popel AS. A numerical study of the shape of the surface separating flow into branches in microvascular bifurcations. *ASME J Biomech Eng* 1992;114:398–405.
- [65] Enden G, Popel AS. A numerical study of plasma skimming in small vascular bifurcations. *J Biomech Eng* 1994;119:79–88.
- [66] Jodal M, Lundgren O. Plasma skimming in the intestinal tract. *Acta Physiol Scand* 1970;80:50–60.
- [67] Johnson PC. Red cell separation in the mesenteric capillary network. *Am J Physiol* 1971;221:99–104.
- [68] Schmid-Schönbein GW, Skalak R, Usami S, Chien S. Cell distribution in capillary networks. *Microvasc Res* 1980;19:18–44.
- [69] Klitzman B, Johnson PC. Capillary network geometry and red cell distribution in hamster cremaster muscle. *Am J Physiol* 1982;242:H211–9.
- [70] Mchedlishvili G, Varazashvili M. Flow conditions of red cells and plasma in microvascular bifurcations. *Biorheology* 1982;19:613–20.
- [71] Pries AR, Ley K, Claßen M, Gaetgens P. Red cell distribution at microvascular bifurcations. *Microvasc Res* 1989;38:81–101.
- [72] Cokelet GR. Blood flow through arterial microvascular bifurcations. In: Popel AS, Johnson PC, eds. *Microvascular Networks: Experimental and Theoretical Studies*. Basel: Karger, 1986:155–67.
- [73] Chien S, Tvetenstrand CD, Farrell Epstein MA, Schmid-Schönbein GW. Model studies on distributions of blood cells at microvascular bifurcations. *Am J Physiol* 1985;248:H568–76.
- [74] Perkkio J, Hokkanen J, Keskinen R. Theoretical model of phase separation of erythrocytes, platelets, and plasma at branches. *Med Phys* 1986;13:882–6.
- [75] Audet DM, Olbricht WL. The motion of model cells at capillary bifurcations. *Microvasc Res* 1986;33:377–96.
- [76] Zweifach BW. Quantitative studies of microcirculatory structure and function. I. Analysis of pressure distribution in the terminal vascular bed in cat mesentery. *Circ Res* 1974;34:843–57.
- [77] Zweifach BW. Quantitative studies of microcirculatory structure and function. II. Direct measurement of capillary pressure in splanchnic mesenteric vessels. *Circ Res* 1974;34:858–66.
- [78] Zweifach BW, Lipowsky HH. Quantitative studies of microcirculatory structure and function. III. Microvascular hemodynamics of cat mesentery and rabbit omentum. *Circ Res* 1977;41:380–90.
- [79] Popel AS. Effect of heterogeneity of capillary flow on the capillary hematocrit. *Proc Am Soc Mech Eng Appl Mech Div* 1979;32:83–4.
- [80] Vicaut E. Statistical estimation of parameters in microcirculation. *Microvasc Res* 1986;32:244–7.
- [81] Pries AR, Secomb TW, Gaetgens P. Structure and hemodynamics of microvascular networks: heterogeneity and correlations. *Am J Physiol* 1995;269:H1713–H1722.
- [82] Renkin EM. Regulation of the microcirculation. *Microvasc Res* 1985;30:251–63.
- [83] Duling BR, Sarelius IH, Jackson WF. A comparison of microvascular estimates of capillary blood flow with direct measurements of total striated muscle flow. *Int J Microcirc Clin Exp* 1982;1:409–24.
- [84] Honig CR, Gayeski TEJ. Correlation of O<sub>2</sub> transport on the micro and macro scale. *Int J Microcirc Clin Exp* 1982;1:367–80.
- [85] Pries AR, Ley K, Gaetgens P. Generalization of the Fahraeus principle for microvessel networks. *Am J Physiol* 1986;251:H1324–32.
- [86] Levin M, Dawant B, Popel AS. Effect of dispersion of vessel diameters and lengths in stochastic networks. II. Modeling of microvascular hematocrit distribution. *Microvasc Res* 1986;31:223–34.
- [87] Sarelius IH, Duling BR. Direct measurement of microvessel hematocrit, red cell flux, velocity and transit time. *Am J Physiol* 1982;243:H1018–26.
- [88] Klitzman B, Duling BR. Microvascular hematocrit and red cell flow in resting and contracting striated muscle. *Am J Physiol* 1979;237:H481–90.
- [89] Keller MW, Damon DN, Duling BR. Determination of capillary tube hematocrit during arteriolar microperfusion. *Am J Physiol* 1994;252:H494–503.
- [90] Pries AR, Gaetgens P. Dispersion of blood cell flow in microvascular networks. In: Lee JS, Skalak TC, eds. *Microvascular Mechanics. Hemodynamics of Systemic and Pulmonary Microcirculation*. New York: Springer, 1989:50–64.
- [91] Lipowsky HH, McKay CB, Seki J. Transit time distribution of blood flow in the microcirculation. In: Lee JS, Skalak TC, eds. *Microvascular Mechanics. Hemodynamics of Systemic and Pulmonary Microcirculation*. New York: Springer-Verlag, 1989:13–27.
- [92] Crystal GJ, Salem MR. Blood volume and hematocrit in regional circulations during isovolemic hemodilution in dogs. *Microvasc Res* 1989;37:237–40.
- [93] Popel AS. Network models of peripheral circulation. In: Skalak R, Chien S, eds. *Handbook of Bioengineering*. New York: McGraw-Hill, 1987:20.1–24.
- [94] Lipowsky HH, Zweifach BW. Network analysis of microcirculation of cat mesentery. *Microvasc Res* 1974;7:73–83.
- [95] Fenton BM, Zweifach BW. Microcirculatory model relating geometrical variation to changes in pressure and flow rate. *Ann Biomed Eng* 1981;9:303–21.
- [96] Fenton BM, Wilson DW, Cokelet GR. Analysis of the effects of

- measured white blood cell entrance times on hemodynamics in a computer model of a microvascular bed. *Pflügers Arch Eur J Physiol* 1985;403:396–401.
- [97] Warnke KC, Skalak TC. The effects of leukocytes on blood flow in a model skeletal muscle capillary network. *Microvasc Res* 1990;40:118–36.
- [98] Dawant B, Levin M, Popel AS. Effect of dispersion of vessel diameters and lengths in stochastic networks. I. Modeling of micro-circulatory flow. *Microvasc Res* 1986;31:203–22.
- [99] Pries AR, Secomb TW, Gaehtgens P. Relationship between structural and hemodynamic heterogeneity in microvascular networks. *Am J Physiol* 1996; 270: H545–H553.
- [100] Murray CD. The physiological principle of minimum work. I. The vascular system and the cost of blood volume. *Proc Natl Acad Sci USA* 1926;12:207–14.
- [101] Kamiya A, Bukhari R, Togawa T. Adaptive regulation of wall shear stress optimizing vascular tree function. *Bull Math Biol* 1984;6:27–137.
- [102] Mayrovitz HN, Roy J. Microvascular blood flow: evidence indicating a cubic dependence on arteriolar diameter. *Am J Physiol* 1983;245:H1031–8.
- [103] Langille BL. Remodeling of developing and mature arteries: endothelium, smooth muscle, and matrix. *J Cardiovasc Pharmacol* 1993;21(suppl 1):S11–7.
- [104] Price RJ, Skalak TC. Circumferential wall stress as a mechanism for arteriolar rarefaction and proliferation in a network model. *Microvasc Res* 1994;47:188–202.
- [105] Pries AR, Secomb TW, Gaehtgens P. Design principles of vascular beds. *Circ Res* 1995;77:1017–1023.